

Article

A novel piezoelectric ultrasonic biological micro-dissection device based on flexure mechanism for suppressing vibration

Haibo Huang¹, Yifan Pan¹, Yan Pang¹, Hao Shen¹, Xiwei Gao¹, Yichen Zhu^{2,*}, Liguao Chen^{1,*} and Lining Sun^{1,3}

¹ School of Mechanical and Electric Engineering, Jiangsu Provincial Key Laboratory of Advanced Robotics, Soochow University, Suzhou, 215123, China; hbhuang@suda.edu.cn(H.H.); yfpannes@stu.suda.edu.cn(Y.P.); 20205229040@stu.suda.edu.cn(Y.P.); 20194029003@stu.suda.edu.cn(H.S.); XiweiGAO@hotmail.com(X.G.); linsun@hit.edu.cn(L.S.)

² Cambridge-Suda Genomic Resource Center, Soochow University, Suzhou, 215123, China,

³ State Key Laboratory of Robotics & Systems, Harbin Institute of Technology, Harbin, China,

* Correspondence: zyc0728@suda.edu.cn; Tel.: +86-18012782002(Y.Z.); chenliguo@suda.edu.cn; Tel: +86-15995831155(L.C.)

Abstract: Biological micro-dissection has a wide range of applications in the field of molecular pathology. The current laser-assisted dissection technology is expensive, and laser radiation can lead to sample contamination. As an economical and pollution-free micro-dissection method, piezoelectric ultrasonic micro-dissection has a wide application prospect. However, the performance of the current piezoelectric ultrasonic micro-dissection technology is unsatisfactory. In this paper, a novel piezoelectric ultrasonic micro-dissection device based on a flexure mechanism is proposed in order to solve the problems of low dissecting precision and excessive wear of the dissecting needle caused by the harmful lateral vibration of the current piezoelectric ultrasonic micro-dissection device. By analyzing the flexibility of flexure hinge, the type of flexure beam and the optimal design parameters are determined. Through comparing the harmonic response simulation analysis of the micro-dissection device based on a flexure mechanism and the traditional micro-dissection device without the flexure mechanism, the newly designed micro-dissection device achieves the best vibration effect when the driving frequency is 28kHz, compared with the traditional micro-dissection device, the lateral vibration suppression effect is improved by 68%. Then, based on the 3D printing technology, a prototype of a novel micro-dissection device was produced, and its performance was tested. It was found that the flexure mechanism did indeed suppress the lateral vibration of the needle tip. Finally, the experiments of 5μm thick paraffin-embedded rat liver sections were carried out, and the effects of different dissecting parameters on the dissecting effect were analyzed, and the optimal dissecting parameters were obtained. By comparing the dissecting effects of the tissue sample and the wear condition of the needle tip between the novel micro-dissection device and the traditional micro-dissection device under their optimal dissecting parameters, it is proved that the suppression of harmful lateral vibration not only significantly improves the dissecting effect, but also improves the service life and durability of the dissecting needle, which is beneficial to reduce the equipment costs.

Keywords: Micro-dissection, Ultrasonic vibration, Flexure-guided, Tissue section

1. Introduction

Micro-dissection technology refers to the selective acquisition of single cells or cell groups from biological tissue slices through micromanipulation systems, separating them from surrounding tissues, and collecting the separated cells for subsequent analysis [1,2]. Micro-dissection has been widely used in the analysis of tumor molecular heterogeneity [3], cell mutation [4], and chromosome

structure analysis [5]. With the continuous development of technology, a variety of different methods have emerged for micro-dissection, including direct manual micro-dissection [6], laser-capture-micro-dissection[7-9] and piezoelectric ultrasonic dissection[10-13].

Direct manual micro-dissection has low precision [14], poor repeatability, and high technical requirements for operators, so it is only suitable for large-area dissection. Laser-capture- micro-dissection technology can quickly capture more target tissues from a large number of research materials, and it is currently the most widely used dissecting method[15].Laser-capture-micro-dissection has been widely used in the analysis of pathological tissues with its advantages of high precision and rapid tissue separation. However, this technique requires special equipment, which is expensive, and may potentially cause contamination from laser radiation during cell capture and separation [16].

Compared with laser dissection technology, piezoelectric ultrasonic micro-dissection technology uses a piezoelectric actuator to drive the dissecting needle to do high-frequency vibration[17]. Therefore, no matter in which direction you dissect, the needle tip is like a sharp saw, which can cleanly separate the cells in the target area without contaminating the sample tissue due to laser radiation and infrared heating. In addition, piezo-power micro-dissection(PPMD) technology does not require expensive special equipment[18] and can be afforded by ordinary laboratories.

However, the current PPMD dissection device has some shortcomings. During the working process of the dissection device, piezoelectric ceramics will not only generate the axial vibration required for dissection, but also generate the lateral vibration which is harmful to the dissection. Excessive lateral vibration will result in uneven dissecting edge and greatly reduce the dissecting precision, and also accelerate the wear of the dissecting needle, making the dissection ineffective. Therefore, how to effectively suppress the lateral vibration is the key to further improve the dissecting effect of PPMD.

Aiming at the problems of low dissecting precision and excessive wear of the dissecting needle caused by the large harmful lateral vibration of the current piezoelectric ultrasonic micro-dissection device. In this paper, a novel piezoelectric ultrasonic micro-dissection device based on flexure mechanism is proposed. It can effectively filter and absorb the vibration energy generated by piezoelectric actuator, retain the axial vibration that is beneficial to dissecting, and suppress the lateral vibration which is harmful to dissecting. Firstly, the type of flexure beam and the optimal design parameters of the flexure mechanism are determined by theoretical analysis. Through the finite element simulation analysis, the harmonic response comparative analysis was carried out with the traditional piezoelectric micro-dissection device without integrated flexure vibration damping structure. The simulation results show that the dissection device designed in this paper has the best vibration effect at 28kHz, and its spatial lateral amplitude evaluation value is 1.59 μm while the dissection device with traditional structure has an optimal spatial lateral amplitude evaluation value of 5.09 μm . Lateral amplitude suppression effect increased by 68%. Based on 3D printing technology, a prototype of the new type of micro-dissection device was made, and its performance was tested. The experimental results show that the dissection device based on the flexure mechanism had no obvious lateral vibration of the tip under the optimal vibration frequency, and the lateral vibration suppression effect was obvious. Finally, the experiments of 5 μm thick paraffin-embedded rat liver sections were carried out, and the effects of different dissecting methods, different driving voltage, different dissecting speed, different dissecting frequency, different dissecting angle and other parameters on the dissecting effect were analyzed, through repeated experiments and comparisons, the optimal dissecting parameters are obtained. When the dissection device works at 28kHz, the driving voltage is 12V, the dissecting speed is 100 $\mu\text{m/s}$, and the dissecting angle is 45°, the optimal dissecting effect can be obtained.

2. Structural design

The micro-dissection needle is connected to the piezoelectric actuator with one end fixed and the other free. In the process of micro-dissection, the energy generated by the piezoelectric actuator is transferred to the needle tip over a distance. However, due to certain errors in processing and

assembly, the piezoelectric actuator not only outputs the axial displacement for micro-dissection, but also produces lateral displacement that is harmful to dissecting. These harmful lateral displacements are amplified at the tip of the needle over a certain distance. Excessive lateral vibration will easily blur the dissecting edge during the dissecting process, which will lead to unsatisfactory dissecting effect. Meanwhile, the collision between the tip and the slice base is inevitable, which will also accelerate the wear of the dissecting needle tip and make the dissecting ineffective. Therefore, suppressing the output lateral energy of piezoelectric ceramics is the key to reducing lateral vibration.

2.1. The overall design of the micro-dissection device

Figure 1a. shows a schematic diagram of a traditional micro-dissection device. The traditional piezoelectric micro-dissection device consists of a fixed rod, a piezoelectric actuator, a clamp, a set screw and a dissecting needle. During the dissecting process, the energy generated by the piezoelectric actuator directly acts on the micro-dissection needle, and the energy of the lateral vibration is amplified as the transmission distance increases. Therefore, this structure cannot achieve precise tissue slices, and is only suitable for larger-scale dissecting.

In order to further improve the dissecting effect, a flexure mechanism is introduced into the design of the micro-dissection device. Figure1b. is a schematic diagram and physical diagram of an ultrasonic piezoelectric micro-dissection device based on a flexure mechanism. The ultrasonic piezoelectric micro-dissection device based on a flexure mechanism is composed of a fixed rod, a connecting base, an outer shell, a packaged piezoelectric ceramic, a flexure mechanism and a dissecting needle. In order to facilitate the assembly, the piezoelectric ceramic p-855.11 (5mm×5mm×9mm) of PI company was selected and encapsulated in a stainless steel case with 200N pretension applied. The energy generated by the piezoelectric ceramics is filtered and absorbed by the flexure mechanism and transferred to the dissecting needle, so that it can obtain a less axial vibration, thereby improving the precision of micro-dissection.

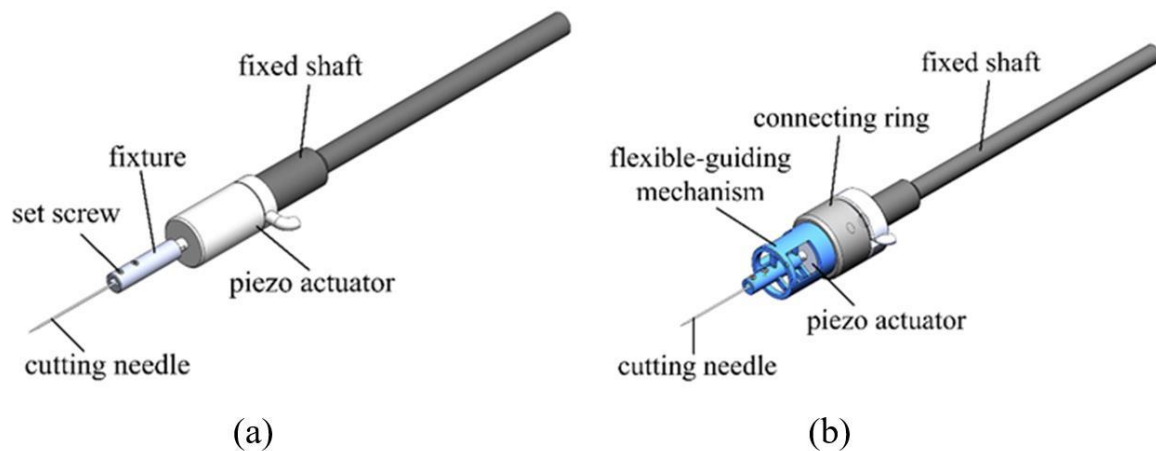


Figure 1. Two piezoelectric ultrasonic micro-dissection devices: (a) Piezoelectric micro-dissection device with traditional structure; (b) Piezoelectric micro-dissection device based on flexure mechanism.

2.2. Design and analysis of flexure hinge

The flexure mechanism is a device that relies on the elastic deformation of the flexure hinge itself to realize movement, force or energy transfer and conversion[19]. Compared with the traditional rigid mechanism, it has the advantages of no gap, no friction, small size, light weight, integrated design and processing, no assembly, high precision, etc. It is widely used in precision positioning and other fields.

In order to reduce the harmful lateral vibration for micro-dissection, the design of flexure hinge is introduced into the micro-dissection device. For the design of the micro-dissection flexure hinge, the flexibility of the output shaft of the micro-dissection device in the Z direction (axial) should be as large as possible, and the flexibility of the output shaft of the micro-dissection device in the X and Y

(lateral) direction should be as small as possible[20]. Several common notched flexure hinges are shown in Figure 2. They are straight-circular flexure hinges, straight-beam flexure hinge, and elliptical flexure hinge. The straight-circular flexure hinge has greater out-of-plane rigidity, but the displacement range is smaller. The straight-beam flexure hinge has a larger displacement range, but the transmission accuracy and outer surface rigidity are poor. The elliptical flexure hinge has a good displacement range and rigidity, but its design calculation and process are more complicated. Considering that the object of micro-dissection is paraffin-embedded pathological tissue slices, and the axial dissecting displacement is small, the straight-circular flexure hinge is selected as the basic unit of the flexure mechanism for design and analysis.

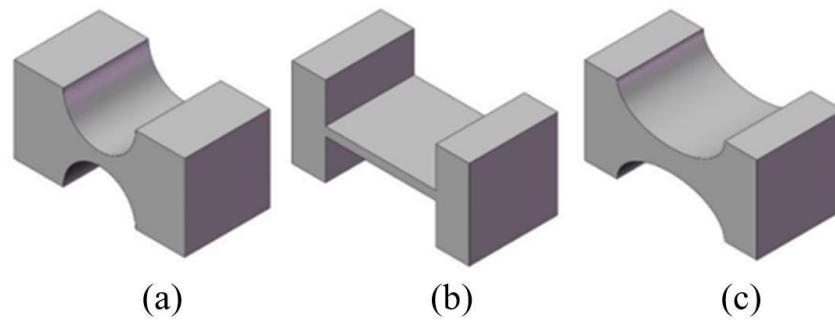


Figure 2. Three common notched flexure hinges: (a) Straight-circular flexure hinge; (b) Straight-beam flexure hinge; (c) Elliptical flexure hinge.

The flexure beam suitable for micro-dissection is composed of two straight-circular-flexure hinges. During the micro-dissection process, it is mainly subjected to two forces. Figure 3a is a simplified diagram of the force analysis of a flexure beam.

First, the output shaft of the micro-dissection device performs linear reciprocating high-frequency vibration along the Y direction, this movement causes the flexure hinge beam joint to be subjected to the force F_y and the moment M_z , causing it to undergo a certain angular deformation α_z around the Z direction and along Y. The direction is linearly deformed by Δ_y .

Secondly, the weak lateral vibration caused by the axial vibration causes the flexure hinge to make a stretching and squeezing movement along the X direction, which mainly causes the flexure hinge to be subjected to a force F_x to produce a linear deformation Δ_x along the X direction.

Therefore, the indexes that affect the main performance parameters of flexure hinge are as follows: 1. The stiffness value of M_z to generate angular deformation along the Z direction under the action of M_z , 2. Under the action of F_y , the flexibility value $\frac{\alpha_z}{F_y}$ of the angular deformation α_z in the Z direction, 3. The stiffness value M_z of linear deformation Δ_y along the Y direction under the action of M_z , 4. The flexibility value F_y of the linear deformation Δ_y along the Y direction under the action of F_y , 5. The flexibility value F_x that produces linear deformation along the X direction under the action of F_x .

The rotational stiffness formula of flexure hinges given by J.M. Paros [21]:

$$K = \frac{2Eb^5\sqrt{t^2}}{9\pi\sqrt{R}}$$

The corner stiffness value is related to the hinge radius R and the minimum hinge distance t . When R is determined, K increases as t increases. Conversely, when t is determined, K decreases as R increases. In order to improve the axial output accuracy and resolution of the flexure mechanism, $\frac{\alpha_z}{M_z}, \frac{\alpha_z}{F_y}, \frac{\Delta_y}{M_z}, \frac{\Delta_y}{F_y}$ should be as large as possible. At this point, the value of R should be appropriately increased and the value of t should be reduced. In order to improve the anti-interference ability of the flexure mechanism against lateral vibration, $\frac{\Delta_x}{F_x}$ should be as large as possible, at this time, the value of R should be reduced and the value of t should be increased as much as possible. In addition, increasing the width b of the flexure hinge increases the overall rigidity of the flexure mechanism. Therefore, when designing the size of the flexure hinge beam, various parameters need to be adjusted repeatedly.

2.3. Overall design of flexure mechanism

According to the analysis in the previous section, the overall design of the flexure mechanism is carried out. In order to avoid the parasitic movement of the flexure hinge during the deformation process, the flexure hinge is arranged in three dimensions. Through constant size modification and simulation verification, the structure size of the flexure mechanism is finally determined. Table 1. is the size parameters of flexure hinge.

The flexure hinge beams are distributed in a circular array at an angle of 120° with the output shaft as the axis, and three flexure hinges are distributed equidistantly on each column. Figure 3b and c shows the three-dimensional model of the flexure mechanism. The flexure mechanism is divided into two parts, a fixed end and a movable end. The outer casing of the flexure guide mechanism is connected with the micro-dissection device to form a fixed frame. The piezoelectric ceramic output shaft and the output shaft of the flexure mechanism are fixed by a screw connection to form a movable end. In order to avoid the displacement of thread gap between the output shaft of piezoelectric actuator and the pivot shaft in the flexure mechanism, a set screw is used for reinforcement at the connection. The entire flexure mechanism is made of 316L stainless steel by 3D printing, and the finished flexure mechanism is shown in Figure 3d.

Table 1. Dimensional parameters of the flexure hinge.

R(mm)	t(mm)	l(mm)	b(mm)	h(mm)	flexure number
0.2	0.6	2	2	1	9(3×3)

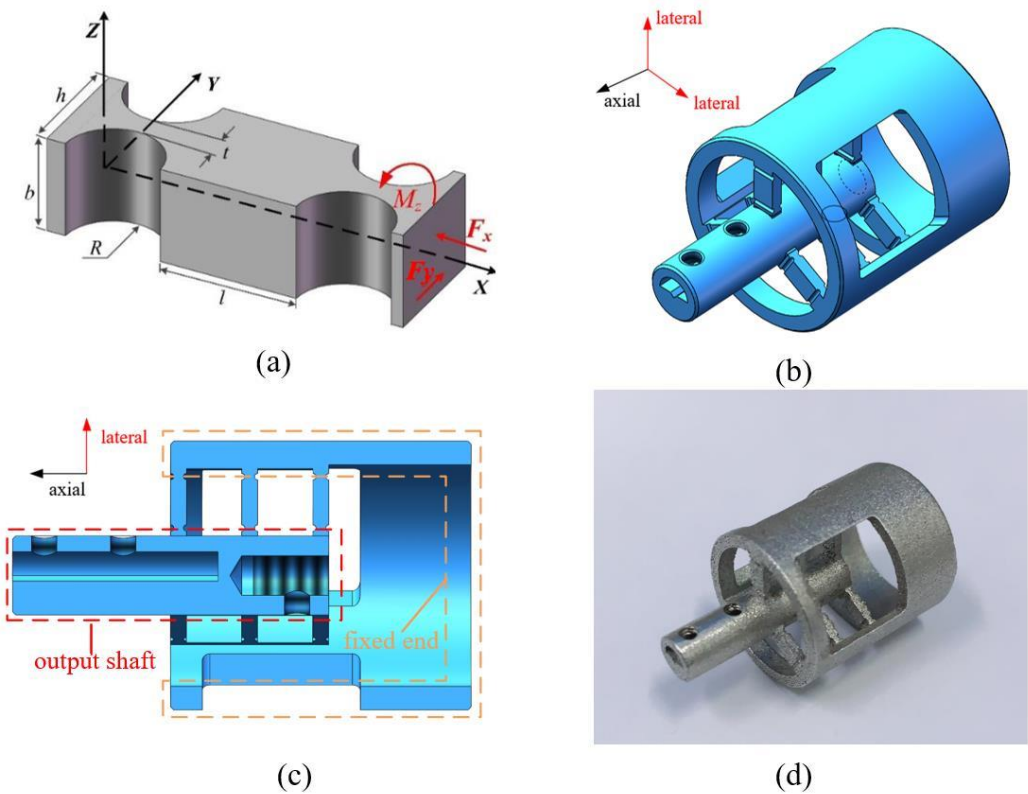


Figure 3. Optimized design and production process of flexure mechanism: (a) Schematic diagram of flexure hinge; (b) Isometric drawing of flexure mechanism; (c) Sectional view of flexure mechanism; (d) Physical picture of flexure mechanism.

3. Simulation analysis

In order to verify the suppression effect of the flexure mechanism on the lateral vibration, a finite element simulation comparison between the micro-dissection device with flexure mechanism and the

traditional micro-dissection device was carried out. Ignoring the threaded fit between the parts of the micro-dissection device, the packaged piezoelectric ceramic is regarded as a whole, and only the shaft end outputs vibration. The material properties of the micro-dissection device are shown in Table 2.

Table 2. Material properties of the micro-dissection device with flexure mechanism.

Components	Material	Density $\rho(\text{g/cm}^3)$	Young's modulus E(GPa)	Poisson's ratio
Dissecting needle	Tungsten	19.35	405	0.28
Flexure mechanism	316L SS	7.89	206	0.3
Packaging Housing、Outer shell	304 SS	7.93	194.02	0.3

3.1. Modal analysis

Since the micro-dissection device generates energy through high-frequency vibration to achieve the purpose of dissecting tissue, it is necessary to perform modal analysis on the entire mechanism before selecting dissecting parameters to avoid resonance with the flexure mechanism or the entire micro-dissection device. Table 3. and Table 4. respectively show the resonant frequency of the micro-dissection device with flexure mechanism and the traditional micro-dissection device within the operating frequency of 20kHz-30kHz.

Table 3. Resonant frequency of the micro-dissection device with flexure mechanism.

Modal	1	2	3
Frequency(kHz)	22.304	22.557	29.633

Table 4. Resonant frequency of the traditional micro-dissection device.

Modal	1	2	3	4	5	6	7
Frequency(kHz)	21.64	23.012	23.648	27.646	27.936	28.923	29.017

3.2. Harmonic response analysis

In order to obtain the displacement of the tip of the two dissection devices under high-frequency vibration, the harmonic response analysis was carried out. A simple harmonic dynamic load of $2\mu\text{m}$ in the axial direction and $1\mu\text{m}$ in the lateral direction was respectively applied to the micro-dissection device with flexure mechanism and the traditional micro-dissection device, the amplitude of the displacement of the two micro-dissection devices varies with frequency as shown in Figure 4.

Figure 4a. shows the variation curves of axial vibration amplitude with frequency of two kinds of micro-dissection devices, As can be seen from Figure 4a, within the working frequency range, the axial output displacement of the traditional micro-dissection device varies greatly with the frequency and is obviously non-linear, which is easy to cause a sudden increase in the amplitude of the dissecting needle tip and thus damage the experimental equipment. Therefore, it should be avoided as far as possible. The micro-dissection device based on the flexure mechanism has a certain amplitude jump at 24.5kHz and 25.5kHz, and can maintain good linearity at other frequency.

Figure 4b. shows the variation curve of lateral vibration amplitude along with frequency on the X-direction component of two kinds of micro-dissection devices. It can be seen from the figure that the lateral vibration of the needle tip of the traditional micro-dissection device in the range of 20-26.5kHz is smaller than that of the micro-dissection device with the flexure mechanism. In the range

of 26.5kHz-30kHz, the lateral vibration amplitude of the micro-dissection device with flexure mechanism is smaller than that of the micro-dissection device with non-flexure mechanism.

Figure 4c. shows the variation curve of the lateral vibration amplitude of the two micro-dissection devices in the Y-direction component with frequency, the variation law is similar to that of the previous section. The lateral vibration of the needle tip in the range of 20-26 kHz of the traditional micro-dissection device is smaller than that of the micro-dissection device with flexure mechanism. In the range of 26.5kHz-29.5kHz, the lateral vibration amplitude of the micro-dissection device with flexure mechanism is smaller than that of the micro-dissection device with non-flexure mechanism.

Since lateral vibration is a physical quantity in a space, define the numerical value of lateral vibration in space as $A_o = \sqrt{A_x^2 + A_y^2}$, where A_x is the lateral vibration amplitude of the dissecting needle in the X-direction component, and A_y is the lateral vibration amplitude of the dissecting needle in the Y-direction component.

Figure 4d. shows the variation curve of the lateral vibration amplitude with frequency in the space of two types of micro-dissection devices. It can be seen from the figure that when the micro-dissection device based on the flexure mechanism works in the range of 26-29.5kHz, its lateral vibration is significantly smaller than that of the traditional micro-dissection device.

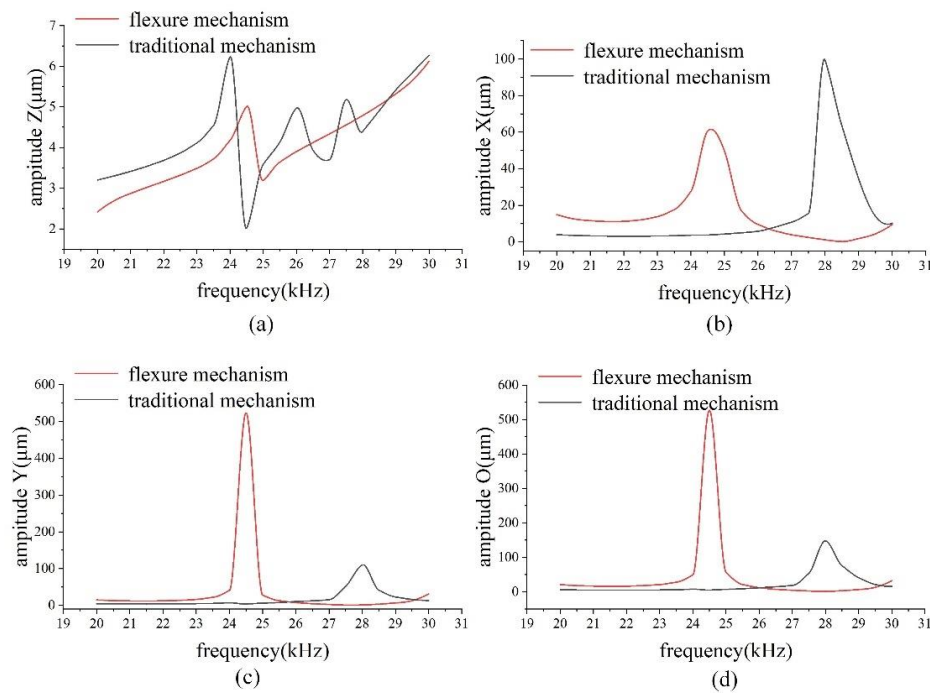


Figure 4. Harmonic response analysis of the needle tip vibration of the micro-dissection device: (a) The frequency response curve of the vibration amplitude in the axial Z direction of the two models; (b) The frequency response curve of the vibration amplitude in the lateral X direction of the two models; (c) Frequency response curve of the vibration amplitude in the lateral Y direction of the two models; (d) The frequency response curve of the overall vibration amplitude of the two models.

In the entire working frequency range, the minimum lateral vibration amplitude of the micro-dissection device with flexure mechanism is much smaller than the minimum lateral vibration amplitude of the traditional mechanism micro-dissection device. The minimum value of the lateral vibration of the micro-dissection device with flexure mechanism appears around 28kHz, at this time $A_x = 1.13\mu\text{m}$, $A_y = 1.12\mu\text{m}$, the evaluation value of lateral vibration in space is $A_o = 1.59\mu\text{m}$ while the minimum value of the lateral vibration of the traditional micro-dissection device appears around 22kHz, at this time $A_x = 3.11\mu\text{m}$, $A_y = 4.03\mu\text{m}$, and the evaluation value of the lateral vibration in

space is $A_0 = 5.09\mu\text{m}$. Figure 5. shows the deformation cloud diagrams of the two micro-dissection devices under optimal vibration conditions.

Through the above analysis, it can be seen that the flexure mechanism dissection device has higher dissecting precision, which is conducive to the realization of high-precision micro-dissection. The optimal dissecting performance of the micro-dissection device based on flexure mechanism is better than that of the traditional micro-dissection device.

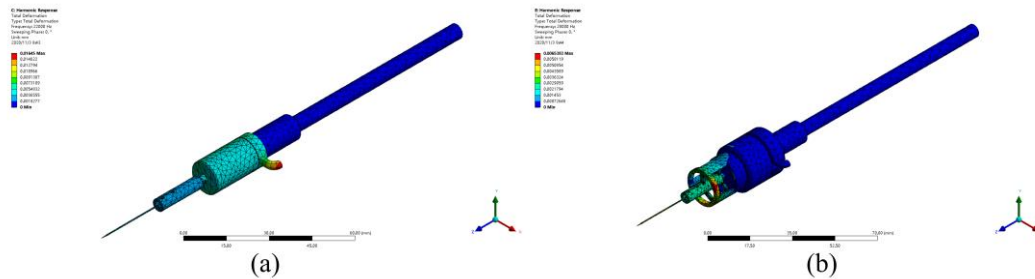


Figure 5. Deformation nephogram under optimal parameters of the two devices: (a) Deformation nephogram of the micro-dissection device with flexure mechanism under optimal vibration conditions; (b) Deformation nephogram of traditional structure micro-dissection device under optimal vibration conditions.

4. Experiment and discussion

4.1 Flexure mechanism vibration test

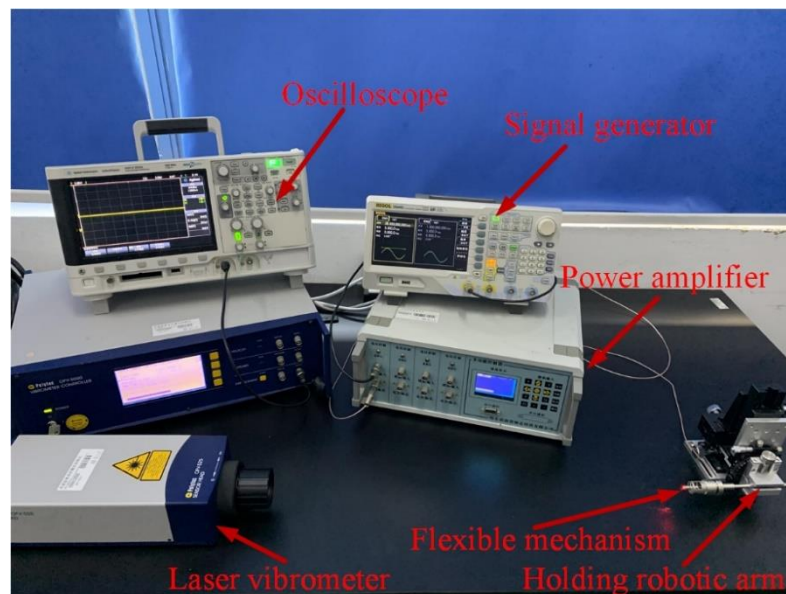


Figure 6. Vibration test platform for the output shaft of the micro-dissection device with flexure mechanism.

In order to determine the suppression effect of the flexure mechanism on the lateral vibration, a laser vibration measurement comparison experiment was carried out on the output shaft of the traditional micro-dissection device and the micro-dissection device with flexure mechanism.

The experimental platform is shown in Figure 6. The test platform is composed of Laser Doppler Vibrometer (OFV-525, OFV-5000, Polytec), signal generator (DG4062, Agilent technologies Inc), piezoelectric power amplifier (RHVD, Harbin Soluble Core Technology Co) and signal generator (DSO-X 2022A, RIGOL Technologies Inc). The laser light emitted by the vibrometer is reflected back

through the output shaft of the dissecting needle, and the vibrometer converts the reflected light signal into an electrical signal, which is finally displayed on the oscilloscope. Through data conversion, the electrical signal is finally converted into the displacement information of the output shaft.

A driving voltage of 8V was applied to the piezoelectric ceramics to test its response between 20kHz-30kHz. The test results were shown in the Figure 7.

It can be seen from Figure 7. that the vibration amplitude of the output shaft of the traditional micro-dissection device fluctuates greatly, and the output shaft of the micro-dissection device with flexure mechanism is basically linear. Under the lower frequency excitation (20-28kHz), the traditional micro-dissection device structure has a smaller lateral amplitude than the micro-dissection device with flexure mechanism. At 28-30kHz, the lateral vibration amplitude of the output shaft of the micro-dissection device with flexure mechanism is smaller than that of the traditional structure micro-dissection device.

In the working frequency range, the minimum lateral vibration amplitude of the output shaft of the micro-dissection device with flexure mechanism is much smaller than the lateral vibration amplitude of the output shaft of the traditional micro-dissection device. Therefore, the introduction of the flexure mechanism will have a positive meaning for improving the micro-dissection performance. The optimal vibration conditions of the two structures are shown in Table 5.

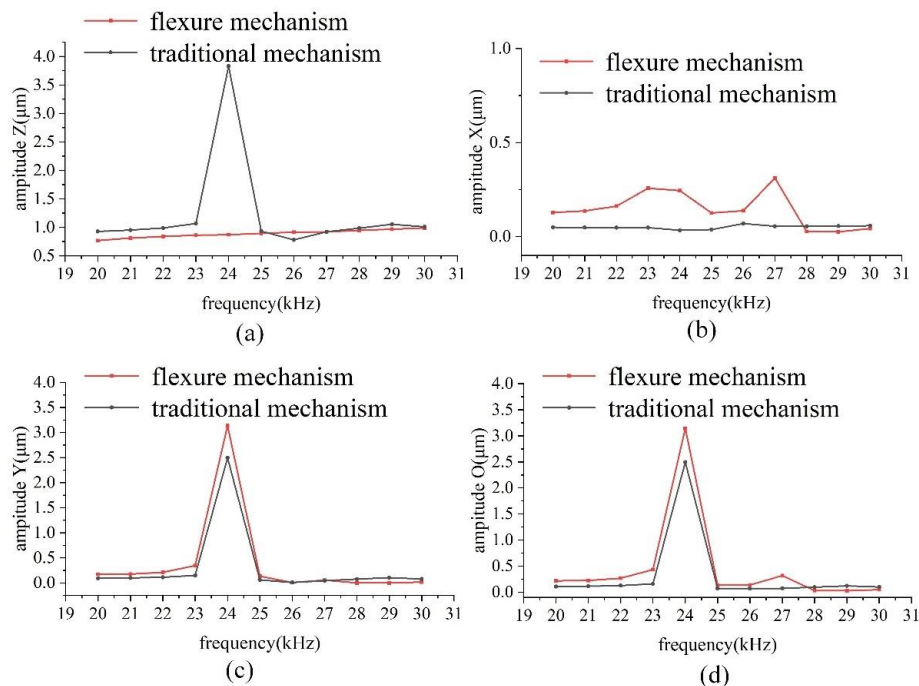


Figure 7. Vibration test of output shaft of the micro-dissection device: (a) The frequency response curve of the vibration amplitude in the axial Z direction of the output shaft of the two structures; (b) The frequency response curve of the vibration amplitude in the lateral X direction of the output shaft of the two structures; (c) The frequency response curve of the vibration amplitude in the lateral Y direction of the output shaft of the two structures; (d) The frequency response curve of the vibration amplitude of the output shaft of the two structures in space.

Table 5. The optimal vibration parameters of the output shaft of the two structures.

	Frequency(kHz)	A_z (μm)	A_x (μm)	A_y (μm)	A_o (μm)
traditional mechanism	26	0.779	0.009	0.069	0.070
flexure mechanism	28	0.947	0.002	0.027	0.027

4.2 Dissecting needle vibration test

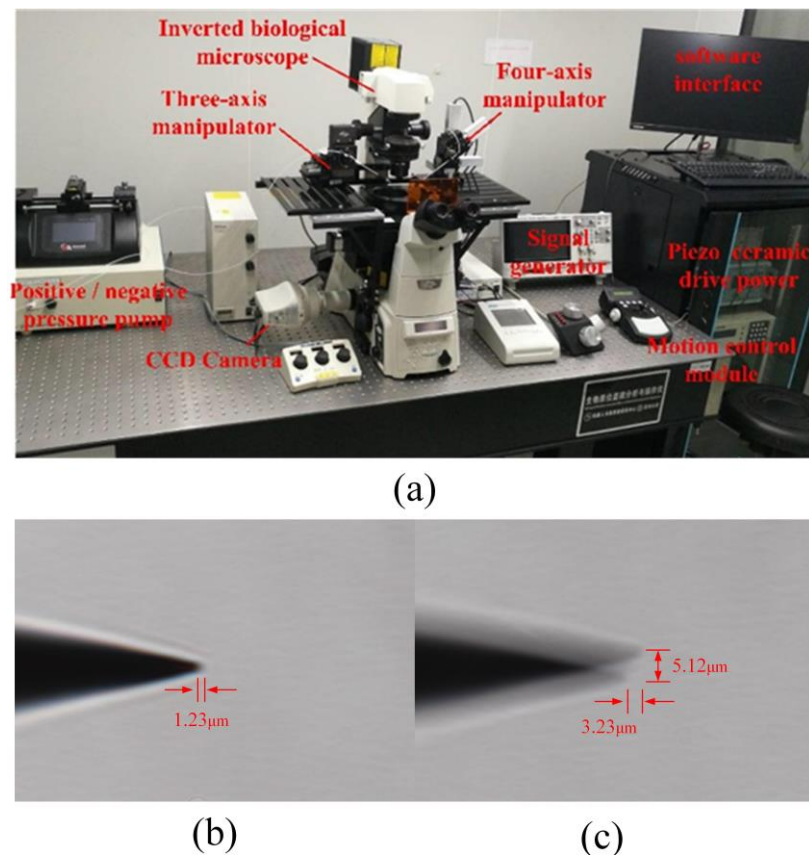


Figure 8. Dissecting needle tip vibration test: (a) The experiment platform; (b) The vibration of the micro-dissection device with flexure mechanism when the lateral vibration is minimal; (c) The vibration of traditional micro-dissection device when lateral vibration is minimum.

Since the diameter of the dissecting needle tip is only $1\mu\text{m}$, it is difficult for laser vibrometers to measure the vibration of a needle tip. Therefore, by observing the residual image of the dissecting tool tip vibration under microscopic vision, the actual vibration of the dissecting tool tip can be determined. The experimental platform shown in Figure 8. was established. The micro-dissection device is installed on the high-precision manipulator on the left side of the micromanipulation experiment platform, and the angle with the horizontal plane is 30° .

Apply a 10V sinusoidal excitation voltage to the piezoelectric ceramics of the two micro-dissection devices, and test their vibration within 20-30kHz.

The stable lateral amplitude of the tip of the traditional micro-dissection device in the test frequency range is $4.87\mu\text{m} \sim 8.96\mu\text{m}$, and the minimum lateral vibration occurs around 22.5kHz. At this time, the axial vibration is about $3.23\mu\text{m}$ and the lateral vibration is about $4.87\mu\text{m}$.

The micro-dissection device with flexure mechanism designed in this paper has a stable lateral amplitude of $0 \sim 6.76\mu\text{m}$ in the test frequency range, and the minimum lateral vibration occurs near 28kHz. At this time, the axial vibration amplitude is about $1.23\mu\text{m}$, and the lateral vibration is almost 0. It is difficult to observe the magnitude of the lateral vibration through microscopic vision. Figure 8b and c. shows the vibration of the two micro-dissection devices under microscopic vision.

It can be seen from the experimental results that the flexure mechanism has a certain suppression effect on both lateral vibration and axial vibration of the needle tip. Under the same driving voltage, the micro-dissection based on the flexure mechanism has a smaller transverse vibration amplitude. Therefore, the micro-cutter based on the flexure mechanism has better dissecting precision.

4.3 Tissue slice dissecting experiment

In order to verify the actual performance of the designed micro-dissection device, a dissecting experiment was performed on a 5 μ m thick rat liver slice. Use different dissecting methods, different driving voltages, different dissecting speeds, different dissecting frequency, and different dissecting angles to compare and find the optimal dissecting parameters. Figure 10. show the experimental platform for tissue section dissecting.

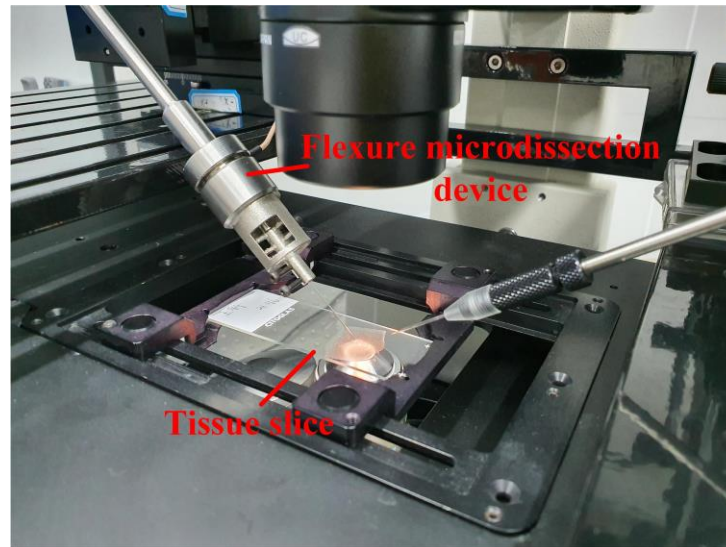


Figure 9. Experimental platform for tissue section dissecting.

Firstly, vibration-free dissecting and ultrasonic dissecting were used to dissect the tissue slices. The dissecting effect is shown in Figure 10a. By observing the two dissecting tracks, we can find that the width of the dissecting track obtained by adopting the vibration-free mechanical dissecting method is not uniform, and there is a phenomenon of local tissue peeling, accompanied by a large number of chips and folds, so the dissecting effect is poor. In contrast, the path dissected by ultrasonic vibration is smoother and more completely separated from the surrounding tissue.

Next, the ultrasonic vibration dissecting method was used to dissect the tissue slices. The main factors affecting the dissecting effect include dissecting angle, driving voltage, dissecting speed and driving frequency.

When the driving sinusoidal voltage on piezoelectric ceramics is 4V, 8V and 12V respectively, the dissecting effect is shown in Figure 10c. From the experimental results, we can see that when the driving voltage is small, the energy generated by ultrasonic vibration is small, so the dissecting track presents a similar effect to mechanical dissection. As the driving voltage increases, the dissecting effect gradually improves. However, when the driving voltage is too large, a larger lateral amplitude will be generated, which will not only affect the dissecting effect, but also accelerate the wear of the dissecting needle. Therefore, it is not advisable to use excessive driving voltage.

Dissecting speed is also a key factor affecting the quality of ultrasonic dissection. The dissecting speeds of 50 μ m/s, 100 μ m/s and 500 μ m/s were used to dissect the slices for comparison experiments. The experimental results are shown in Figure 10d. When the dissecting speed is slow, the chips tend to adhere to the tip, thus affecting the precision of the dissecting track, and the chips may fall off during the dissecting, affecting the subsequent collection work. When the dissecting speed is too fast, the contact time between the dissecting needle and the tissue is short, and the tissue cannot be separated by sufficient ultrasonic energy, so the dissecting effect is similar to that of mechanical dissecting.

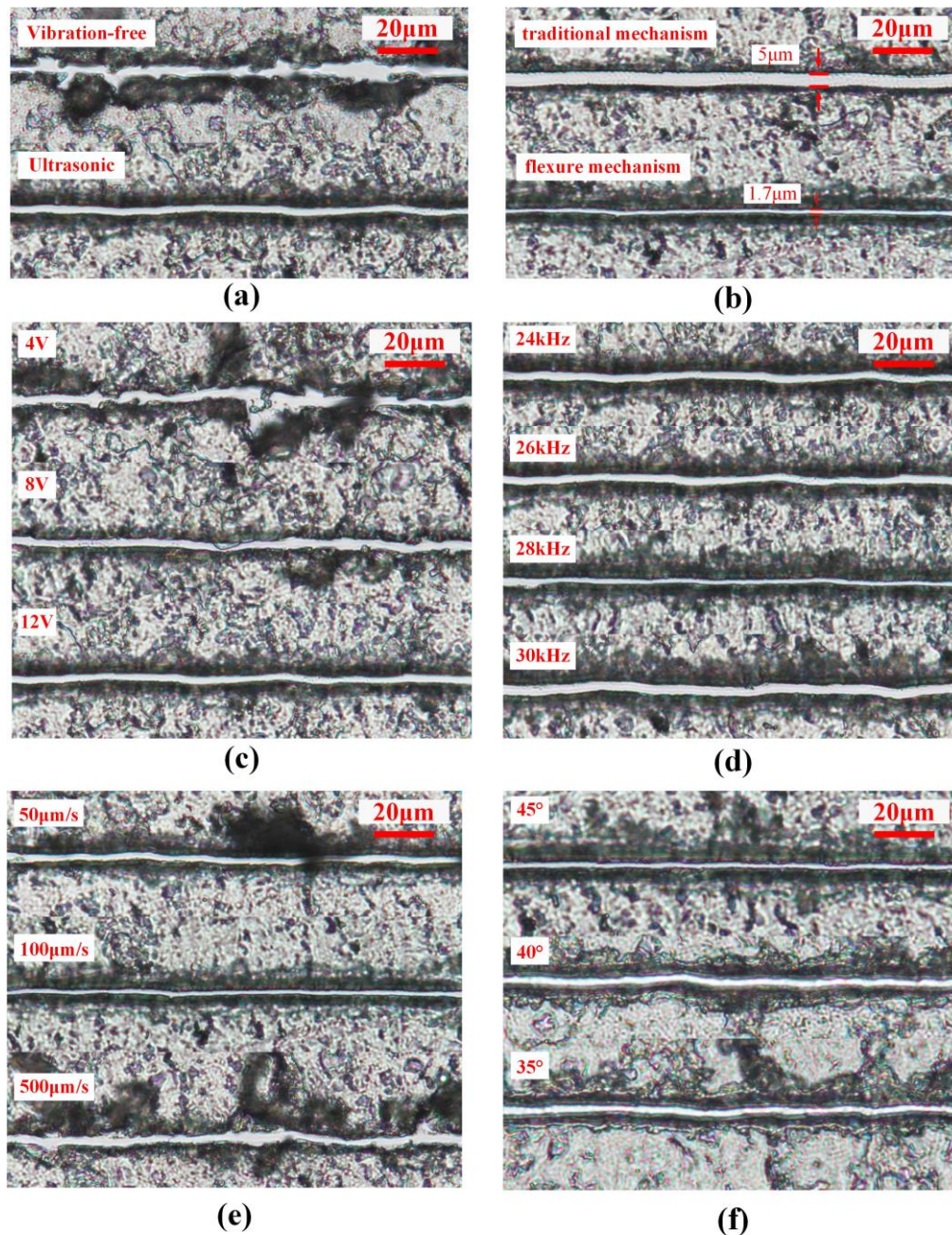


Figure 10. Experimental results of tissue section dissecting under different dissecting parameters: (a) Different dissecting methods; (b) Dissecting effect of two structures; (c) Different drive voltage; (d) Different drive frequency; (e) Different dissecting speed; (f) Different dissecting angles.

The influence of frequency on the dissecting effect is mainly reflected in the dissecting precision. When the appropriate driving voltage, dissecting speed and dissecting angle are selected, different driving frequency can achieve good tissue separation effect. Dissecting experiments were conducted at drive frequency of 24kHz, 26kHz, 28kHz and 30kHz for tissue slices, as shown in Figure 10e. It can be seen from the experimental results that when the micro-dissection device works at 28KHz, the lateral vibration is the smallest and the trajectory is the smallest, which is conducive to the realization of precise tissue dissecting.

The dissecting angle is also one of the main factors that affect the dissecting effect. The liver slices were dissected at 45°, 40°, and 35° respectively. The experimental results are shown in Figure 10f.

When the dissecting needle and the dissected tissue are at an angle of 45° , the dissecting track is clear, the residual tissue is evenly divided, and the dissecting effect is the best.

Through repeated experimental tests, the best dissecting parameters for $5\mu\text{m}$ thick rat liver slices were finally obtained. The best dissecting effect can be obtained when the operating frequency of the system is 28kHz , the driving voltage is 12V , the dissecting speed is $100\mu\text{m/s}$ and the dissecting angle is 45° .

Finally, the micro-dissection device with the traditional mechanism and the micro-dissection device with the flexure mechanism are compared. Through repeated experiments, the optimal dissecting parameters of the micro-dissection device with the traditional mechanism are obtained. The best dissecting effect can be obtained when the micro-dissection device with the traditional mechanism works at 22kHz , the driving voltage is 12V , the dissecting speed is $100\mu\text{m/s}$ and the dissecting angle is 45° . The comparative experimental results of the optimal dissecting parameters of the micro-dissection device with the traditional mechanism and the micro-dissection device with the flexure mechanism are shown in Figure 10b. We can clearly see that the large lateral vibration generated by the traditional dissection device is obvious on the dissecting track. Jagged marks exist at the edge of the track and tissue residues caused by lateral vibration are left on the dissecting track. In contrast, the micro-dissection device with flexure mechanism has finer track, cleaner separation and better dissecting effect.

Excessive lateral vibration will also aggravate the wear of the dissecting needle and make the dissecting effect worse. After 30 times same dissecting tasks, the wear of the two dissecting tips was observed. Figure 11 is the observation picture of the tip deformation under the microscope. It can be seen from the figure that the tip deformation of the micro-dissection device with the traditional mechanism is more serious. Because the flexure mechanism has a good suppressing effect on the lateral vibration, the tip wear is less during dissecting.

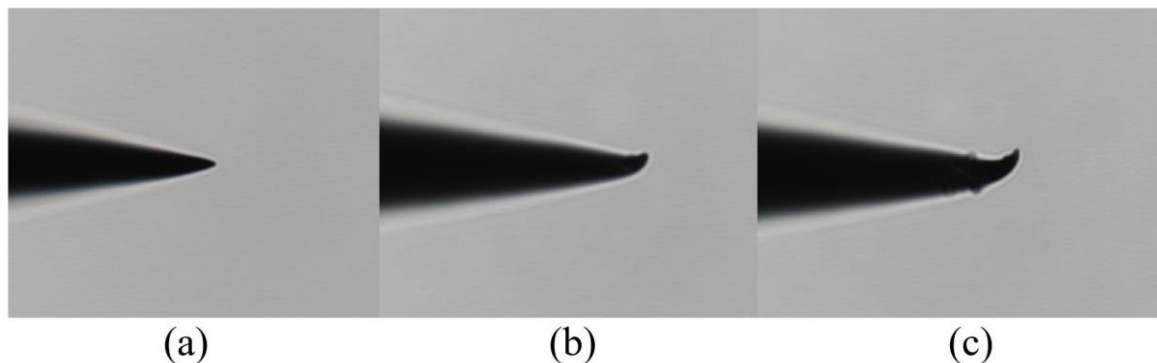


Figure 11. Experimental results of the dissecting needle tip wear: (a) Unused needle tip; (b) Wear condition of tip of the micro-dissection device with flexure mechanism; (c) Wear condition of tip of the micro-dissection device with the traditional mechanism.

5. Conclusion

This paper proposes a high-precision piezoelectric ultrasonic micro-dissection device based on a flexure mechanism. Through the design of the flexure hinge and simulation optimization, the structural design parameters of the dissection device are determined. The newly designed micro-dissection device can significantly reduce the harmful lateral vibration and make the tip vibration more stable, which is proved by simulation and experiment. The influence of driving voltage, dissecting speed, dissecting frequency and dissecting angle on the dissecting effect were investigated through experimental analysis of paraffin sections of rat liver with a thickness of $5\mu\text{m}$. Finally, after repeated experimental analysis, the optimal dissecting parameters are determined. Through the experiment comparison with the traditional micro-dissection device, it is proved that the dissection device based on the flexure mechanism has better dissecting precision and dissecting effect, and improves the service life and durability of the dissecting needle.

Funding: This research was funded by the National Key R&D Program of China (2018YFB1304905), the Natural Science Foundation of Jiangsu Province of China (BK20171215), the Natural Science Foundation of the Jiangsu Higher Education Institutions of China (17KJA460008), and the Suzhou Science and Technology Innovation Policy Funded Project(SCJ [2020] No.45).

Conflicts of Interest: The authors declare no conflict of interest.

References

1. Yamazaki, M.; Hosokawa, M.; Arikawa, K.; Takahashi, K.; Sakanashi, C.; Yoda, T.; Matsunaga, H.; Takeyama, H. Effective microtissue RNA extraction coupled with Smart-seq2 for reproducible and robust spatial transcriptome analysis. *Scientific Reports* **2020**, *10*, 7083.
2. Feng, L.; Hagiwara, M.; Ichikawa, A.; Arai, F. On-Chip Enucleation of Bovine Oocytes using Microrobot-Assisted Flow-Speed Control. *Micromachines* **2013**, *4*, 272-285.
3. Moffitt, R.A.; Marayati, R.; Flate, E.L.; Volmar, K.E.; Loeza, S.G.; Hoadley, K.A.; Rashid, N.U.; Williams, L.A.; Eaton, S.C.; Chung, A.H., et al. Virtual microdissection identifies distinct tumor- and stroma-specific subtypes of pancreatic ductal adenocarcinoma. *Nature genetics* **2015**, *47*, 1168-1178.
4. Oh, S.; Lee, H. Efficiency of EGFR mutation analysis for small microdissected cytological specimens using multitech DNA extraction solution: Efficiency of EGFR Mutation Analysis. *Cancer cytopathology* **2015**, 123.
5. Zlotina, A.; Kulikova, T.; Kosyakova, N.; Liehr, T.; Krasikova, A. Microdissection of lampbrush chromosomes as an approach for generation of locus-specific FISH-probes and samples for high-throughput sequencing. *BMC genomics* **2016**, *17*, 126.
6. Hoffman, D.; Chaffins, M.; Cankovic, M.; Maeda, K.; Meehan, S. Manual microdissection technique in a case of subcutaneous panniculitis-like T-cell lymphoma: a case report and review. *Journal of cutaneous pathology* **2012**, *39*, 769-772.
7. De Marchi, T.; Braakman, R.B.; Stingl, C.; van Duijn, M.M.; Smid, M.; Foekens, J.A.; Luijck, T.M.; Martens, J.W.; Umar, A. The advantage of laser-capture microdissection over whole tissue analysis in proteomic profiling studies. *Proteomics* **2016**, *16*, 1474-1485.
8. Dilillo, M.; Pellegrini, D.; Ait-Belkacem, R.; de Graaf, E.L.; Caleo, M.; McDonnell, L.A. Mass Spectrometry Imaging, Laser Capture Microdissection, and LC-MS/MS of the Same Tissue Section. *Journal of Proteome Research* **2017**, *16*, 2993-3001.
9. Emmert-Buck, M.R.; Bonner, R.F.; Smith, P.D.; Chuaqui, R.F.; Zhuang, Z.; Goldstein, S.R.; Weiss, R.A.; Liotta, L.A. Laser capture microdissection. *Science (New York, N.Y.)* **1996**, *274*, 998-1001.
10. Liu, Y.; Zhong, M. A Novel Piezoelectric Micro-Dissection Tool with Ultrasonic Vibration. *Advanced Materials Research* **2011**, 239-242, 1343-1348.
11. Ru, C.; Liu, J.; Pang, M.; Sun, Y. Controlled ultrasonic micro-dissection of thin tissue sections. *Biomedical microdevices* **2014**, *16*, 567-573.
12. Gao, X.; Huang, H.; Chen, L.; Pan, M.; Sun, L. Design and Simulation Optimization of a Novel Oocyte Ultrasonic Micro-dissection Instrument. In Proceedings of 2018 15th International Conference on Control, Automation, Robotics and Vision (ICARCV).
13. Gao, X.; Huang, H.; Chen, L.; Yan, S.; Li, Y.; Sun, L. Research on Single Cell Precision Cutting Technology Based on Piezoelectric Ultrasonic Vibration. In Proceedings of 2018 IEEE International Conference on Robotics and Biomimetics (ROBIO), 12-15 Dec. 2018; pp. 21-26.

14. Moelans, C.B.; de Weger, R.A.; Ezendam, C.; van Diest, P.J. HER-2/neu amplification testing in breast cancer by Multiplex Ligation-dependent Probe Amplification: influence of manual- and laser microdissection. *BMC cancer* **2009**, *9*, 4.
15. Küppers, R.; Schneider, M.; Hansmann, M.L. Laser-based microdissection of single cells from tissue sections and PCR analysis of rearranged immunoglobulin genes from isolated normal and malignant human B cells. *Methods in molecular biology (Clifton, N.J.)* **2013**, *971*, 49-63.
16. McLachlan, J.L.; Smith, A.J.; Cooper, P.R. Piezo-power microdissection of mature human dental tissue. *Archives of oral biology* **2003**, *48*, 731-736.
17. Sun, L.; Wang, H.; Chen, L.; Liu, Y. A novel ultrasonic micro-dissection technique for biomedicine. *Ultrasonics* **2006**, *44 Suppl 1*, e255-260.
18. Meng, Z.; Hai, R.C. Automated and depth-controlled system for tissue dissection. In Proceedings of Biomedical Engineering and Sciences (IECBES), 2012 IEEE EMBS Conference on.
19. Xu, Q. Precision Motion Control of Piezoelectric Nanopositioning Stage With Chattering-Free Adaptive Sliding Mode Control. *IEEE Transactions on Automation Science and Engineering* **2017**, *14*, 238-248.
20. Johnson, W.; Dai, C.; Liu, J.; Wang, X.; Luu, D.K.; Zhang, Z.; Ru, C.; Zhou, C.; Tan, M.; Pu, H., et al. A Flexure-Guided Piezo Drill for Penetrating the Zona Pellucida of Mammalian Oocytes. *IEEE Transactions on Biomedical Engineering* **2018**, *65*, 678-686.
21. Wu, Y.; Zhou, Z. Design of flexure hinges. *Engineering Mechanics* **2002**, *19*, 136-140.